

**Search for the Rare Decays  $J/\psi \rightarrow D_s^- e^+ \nu_e$ ,  
 $J/\psi \rightarrow D^- e^+ \nu_e$ , and  $J/\psi \rightarrow \bar{D}^0 e^+ e^-$**

M. Ablikim<sup>1</sup>, J. Z. Bai<sup>1</sup>, Y. Ban<sup>12</sup>, J. G. Bian<sup>1</sup>, X. Cai<sup>1</sup>, H. F. Chen<sup>17</sup>,  
H. S. Chen<sup>1</sup>, H. X. Chen<sup>1</sup>, J. C. Chen<sup>1</sup>, Jin Chen<sup>1</sup>, Y. B. Chen<sup>1</sup>, S. P. Chi<sup>2</sup>,  
Y. P. Chu<sup>1</sup>, X. Z. Cui<sup>1</sup>, Y. S. Dai<sup>19</sup>, L. Y. Diao<sup>9</sup>, Z. Y. Deng<sup>1</sup>, Q. F. Dong<sup>15</sup>,  
S. X. Du<sup>1</sup>, J. Fang<sup>1</sup>, S. S. Fang<sup>2</sup>, C. D. Fu<sup>1</sup>, C. S. Gao<sup>1</sup>, Y. N. Gao<sup>15</sup>, S. D. Gu<sup>1</sup>,  
Y. T. Gu<sup>4</sup>, Y. N. Guo<sup>1</sup>, Y. Q. Guo<sup>1</sup>, Z. J. Guo<sup>16</sup>, F. A. Harris<sup>16</sup>, K. L. He<sup>1</sup>,  
M. He<sup>13</sup>, Y. K. Heng<sup>1</sup>, H. M. Hu<sup>1</sup>, T. Hu<sup>1</sup>, G. S. Huang<sup>1a</sup>, X. T. Huang<sup>13</sup>,  
X. B. Ji<sup>1</sup>, X. S. Jiang<sup>1</sup>, X. Y. Jiang<sup>5</sup>, J. B. Jiao<sup>13</sup>, D. P. Jin<sup>1</sup>, S. Jin<sup>1</sup>, Yi Jin<sup>8</sup>,  
Y. F. Lai<sup>1</sup>, G. Li<sup>2</sup>, H. B. Li<sup>1</sup>, H. H. Li<sup>1</sup>, J. Li<sup>1</sup>, R. Y. Li<sup>1</sup>, S. M. Li<sup>1</sup>, W. D. Li<sup>1</sup>,  
W. G. Li<sup>1</sup>, X. L. Li<sup>1</sup>, X. N. Li<sup>1</sup>, X. Q. Li<sup>11</sup>, Y. L. Li<sup>4</sup>, Y. F. Liang<sup>14</sup>, H. B. Liao<sup>1</sup>,  
B. J. Liu<sup>1</sup>, C. X. Liu<sup>1</sup>, F. Liu<sup>6</sup>, Fang Liu<sup>1</sup>, H. H. Liu<sup>1</sup>, H. M. Liu<sup>1</sup>, J. Liu<sup>12</sup>,  
J. B. Liu<sup>1</sup>, J. P. Liu<sup>18</sup>, Q. Liu<sup>1</sup>, R. G. Liu<sup>1</sup>, Z. A. Liu<sup>1</sup>, Y. C. Lou<sup>5</sup>, F. Lu<sup>1</sup>,  
G. R. Lu<sup>5</sup>, J. G. Lu<sup>1</sup>, C. L. Luo<sup>10</sup>, F. C. Ma<sup>9</sup>, H. L. Ma<sup>1</sup>, L. L. Ma<sup>1</sup>, Q. M. Ma<sup>1</sup>,  
X. B. Ma<sup>5</sup>, Z. P. Mao<sup>1</sup>, X. H. Mo<sup>1</sup>, J. Nie<sup>1</sup>, S. L. Olsen<sup>16</sup>, H. P. Peng<sup>17b</sup>,  
R. G. Ping<sup>1</sup>, N. D. Qi<sup>1</sup>, H. Qin<sup>1</sup>, J. F. Qiu<sup>1</sup>, Z. Y. Ren<sup>1</sup>, G. Rong<sup>1</sup>, L. Y. Shan<sup>1</sup>,  
L. Shang<sup>1</sup>, C. P. Shen<sup>1</sup>, D. L. Shen<sup>1</sup>, X. Y. Shen<sup>1</sup>, H. Y. Sheng<sup>1</sup>, H. S. Sun<sup>1</sup>,  
J. F. Sun<sup>1</sup>, S. S. Sun<sup>1</sup>, Y. Z. Sun<sup>1</sup>, Z. J. Sun<sup>1</sup>, Z. Q. Tan<sup>4</sup>, X. Tang<sup>1</sup>, G. L. Tong<sup>1</sup>,  
G. S. Varner<sup>16</sup>, D. Y. Wang<sup>1</sup>, L. Wang<sup>1</sup>, L. L. Wang<sup>1</sup>, L. S. Wang<sup>1</sup>, M. Wang<sup>1</sup>,  
P. Wang<sup>1</sup>, P. L. Wang<sup>1</sup>, W. F. Wang<sup>1c</sup>, Y. F. Wang<sup>1</sup>, Z. Wang<sup>1</sup>, Z. Y. Wang<sup>1</sup>,  
Zhe Wang<sup>1</sup>, Zheng Wang<sup>2</sup>, C. L. Wei<sup>1</sup>, D. H. Wei<sup>1</sup>, N. Wu<sup>1</sup>, X. M. Xia<sup>1</sup>,  
X. X. Xie<sup>1</sup>, G. F. Xu<sup>1</sup>, X. P. Xu<sup>6</sup>, Y. Xu<sup>11</sup>, M. L. Yan<sup>17</sup>, H. X. Yang<sup>1</sup>, Y. X. Yang<sup>3</sup>,  
M. H. Ye<sup>2</sup>, Y. X. Ye<sup>17</sup>, Z. Y. Yi<sup>1</sup>, G. W. Yu<sup>1</sup>, C. Z. Yuan<sup>1</sup>, J. M. Yuan<sup>1</sup>, Y. Yuan<sup>1</sup>,  
S. L. Zang<sup>1</sup>, Y. Zeng<sup>7</sup>, Yu Zeng<sup>1</sup>, B. X. Zhang<sup>1</sup>, B. Y. Zhang<sup>1</sup>, C. C. Zhang<sup>1</sup>,  
D. H. Zhang<sup>1</sup>, H. Q. Zhang<sup>1</sup>, H. Y. Zhang<sup>1</sup>, J. W. Zhang<sup>1</sup>, J. Y. Zhang<sup>1</sup>,  
S. H. Zhang<sup>1</sup>, X. M. Zhang<sup>1</sup>, X. Y. Zhang<sup>13</sup>, Yiyun Zhang<sup>14</sup>, Z. P. Zhang<sup>17</sup>,  
D. X. Zhao<sup>1</sup>, J. W. Zhao<sup>1</sup>, M. G. Zhao<sup>1</sup>, P. P. Zhao<sup>1</sup>, W. R. Zhao<sup>1</sup>, Z. G. Zhao<sup>1d</sup>,  
H. Q. Zheng<sup>12</sup>, J. P. Zheng<sup>1</sup>, Z. P. Zheng<sup>1</sup>, L. Zhou<sup>1</sup>, N. F. Zhou<sup>1d</sup>, K. J. Zhu<sup>1</sup>,  
Q. M. Zhu<sup>1</sup>, Y. C. Zhu<sup>1</sup>, Y. S. Zhu<sup>1</sup>, Yingchun Zhu<sup>1b</sup>, Z. A. Zhu<sup>1</sup>, B. A. Zhuang<sup>1</sup>,  
X. A. Zhuang<sup>1</sup>, B. S. Zou<sup>1</sup>

(BES Collaboration)

<sup>1</sup> *Institute of High Energy Physics, Beijing 100049, People's Republic of China*

<sup>2</sup> *China Center for Advanced Science and Technology (CCAST), Beijing 100080, People's Republic of China*

<sup>3</sup> *Guangxi Normal University, Guilin 541004, People's Republic of China*

<sup>4</sup> *Guangxi University, Nanning 530004, People's Republic of China*

<sup>5</sup> *Henan Normal University, Xinxiang 453002, People's Republic of China*

<sup>6</sup> *Huazhong Normal University, Wuhan 430079, People's Republic of China*

<sup>7</sup> *Hunan University, Changsha 410082, People's Republic of China*

<sup>8</sup> *Jinan University, Jinan 250022, People's Republic of China*

<sup>9</sup> *Liaoning University, Shenyang 110036, People's Republic of China*

<sup>10</sup> *Nanjing Normal University, Nanjing 210097, People's Republic of China*

- <sup>11</sup> *Nankai University, Tianjin 300071, People's Republic of China*  
<sup>12</sup> *Peking University, Beijing 100871, People's Republic of China*  
<sup>13</sup> *Shandong University, Jinan 250100, People's Republic of China*  
<sup>14</sup> *Sichuan University, Chengdu 610064, People's Republic of China*  
<sup>15</sup> *Tsinghua University, Beijing 100084, People's Republic of China*  
<sup>16</sup> *University of Hawaii, Honolulu, HI 96822, USA*  
<sup>17</sup> *University of Science and Technology of China, Hefei 230026, People's Republic of China*  
<sup>18</sup> *Wuhan University, Wuhan 430072, People's Republic of China*  
<sup>19</sup> *Zhejiang University, Hangzhou 310028, People's Republic of China*  
<sup>a</sup> *Current address: Purdue University, West Lafayette, IN 47907, USA*  
<sup>b</sup> *Current address: DESY, D-22607, Hamburg, Germany*  
<sup>c</sup> *Current address: Laboratoire de l'Accélérateur Linéaire, Orsay, F-91898, France*  
<sup>d</sup> *Current address: University of Michigan, Ann Arbor, MI 48109, USA*

---

## Abstract

We report on a search for the decays  $J/\psi \rightarrow D_s^- e^+ \nu_e + c.c.$ ,  $J/\psi \rightarrow D^- e^+ \nu_e + c.c.$ , and  $J/\psi \rightarrow \overline{D}^0 e^+ e^- + c.c.$  in a sample of  $5.8 \times 10^7 J/\psi$  events collected with the BESII detector at the BEPC. No excess of signal above background is observed, and 90% confidence level upper limits on the branching fractions are set:  $B(J/\psi \rightarrow D_s^- e^+ \nu_e + c.c.) < 4.8 \times 10^{-5}$ ,  $B(J/\psi \rightarrow D^- e^+ \nu_e + c.c.) < 1.2 \times 10^{-5}$ , and  $B(J/\psi \rightarrow \overline{D}^0 e^+ e^- + c.c.) < 1.1 \times 10^{-5}$ .

PACS: 13.25.Gv, 13.30.Ce

---

## 1 INTRODUCTION

Hadronic, electromagnetic, and radiative decays of the  $J/\psi$  have been widely studied. However there have been few searches for rare weak  $J/\psi$  decay processes. Kinematically, the  $J/\psi$  cannot decay into a pair of charmed  $D$  mesons, but can decay into a single  $D$  meson. Searches for weak decays of  $J/\psi$  to single  $D$  or  $D_s$  mesons provide tests of standard model (SM) theory and serve as a probe of new physics [1], such as TopColor models, the minimal supersymmetric standard model with or without R-parity, and the two Higgs doublet model [2].

The branching fractions of  $J/\psi$  decays to single  $D$  or  $D_s$  mesons are predicted to be about  $10^{-8}$  or smaller [3] in the SM. The flavor changing neutral current (FCNC) process  $c \rightarrow u$  occurs in the standard model only at the loop level where it is suppressed by the GIM mechanism. Fig. 1 shows the dominant Feynman diagrams within the standard model for the decays

$J/\psi \rightarrow D_s^- e^+ \nu_e$ ,  $J/\psi \rightarrow D^- e^+ \nu_e$ , and  $J/\psi \rightarrow \overline{D}^0 e^+ e^-$ . No decay of this type has been observed before. In this paper, we perform a search for the decays  $J/\psi \rightarrow D_s^- e^+ \nu_e$ ,  $J/\psi \rightarrow D^- e^+ \nu_e$ , and  $J/\psi \rightarrow \overline{D}^0 e^+ e^-$  in a sample of  $5.8 \times 10^7 J/\psi$  events collected with the Beijing Spectrometer (BESII) [4] detector at the Beijing Electron-Positron Collider (BEPC) [5]. Throughout this paper the charge conjugate states are implicitly included.

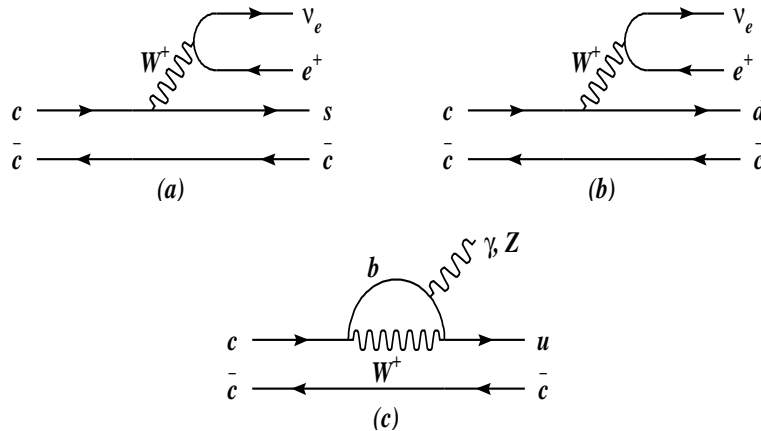


Fig. 1. Typical Feynman diagrams for (a)  $J/\psi \rightarrow D_s^- e^+ \nu_e$ , (b)  $J/\psi \rightarrow D^- e^+ \nu_e$ , and (c)  $J/\psi \rightarrow \overline{D}^0 e^+ e^-$ .

## 2 BESII Detector

BES is a conventional solenoidal magnetic detector that is described in detail in Ref. [6]. BESII is the upgraded version of the BES detector [4]. A 12-layer Vertex Chamber (VC) surrounds the beryllium beam pipe and provides track and trigger information. A forty-layer main drift chamber (MDC) located just outside the VC provides measurements of charged particle trajectories over 85% of the total solid angle; it also provides ionization energy loss ( $dE/dx$ ) measurements which are used for particle identification (PID). A momentum resolution of  $1.78\% \sqrt{1+p^2}$  ( $p$  in GeV/ $c$ ) and a  $dE/dx$  resolution for Bhabha electrons of  $\sim 8\%$  are obtained. An array of 48 scintillation counters surrounding the MDC measures the time of flight (TOF) of charged particles with a resolution of about 200 ps for hadrons. Outside the TOF counters, a 12 radiation length, lead-gas barrel shower counter (BSC), operating in self quenching streamer mode, measures the energies and positions of electrons and photons over 80% of the total solid angle with resolutions of  $\sigma_E/E = 0.21/\sqrt{E}$  ( $E$  in GeV),  $\sigma_\phi = 7.9$  mrad, and  $\sigma_z = 2.3$  cm. Outside the solenoidal coil, which provides a 0.4 T magnetic field over the tracking volume, is an iron flux return that is instrumented with three double-layer muon counters that identify muons with momentum greater than 500 MeV/ $c$ .

In this analysis, a GEANT3-based Monte Carlo program (SIMBES) with detailed consideration of the detector performance is used. The consistency between data and Monte Carlo has been checked in many physics channels from  $J/\psi$  and  $\psi(2S)$  decays, and the agreement is reasonable, as described in detail in Ref. [7].

### 3 Event Selection

Each charged track is required to be well fitted to a helix that is within the polar angle region  $|\cos\theta| < 0.8$  and to originate from the beam interaction region, which is defined to be within 2 cm of the beam line in the transverse plane and within 20 cm of the interaction point along the beam direction. For particle identification, confidence levels ( $CL$ ) are calculated for each particle hypothesis using combined time-of-flight [8] and MDC energy loss information. Pions and kaons are identified by requiring the confidence level for the desired hypothesis to be greater than 0.1% and, further, by requiring the normalized weights, defined as  $CL_\alpha/(CL_\pi+CL_K)$ , where  $\alpha$  denotes the desired particle, to exceed 0.7. For electron identification, the  $dE/dx$ , TOF, and BSC information are combined to form a particle identification confidence level for the electron hypothesis. An electron candidate is required to have  $CL_e > 1.0\%$  and satisfy  $CL_e/(CL_e + CL_\pi + CL_K) > 0.85$ .

An isolated neutral cluster is considered to be a photon candidate when the angle between the nearest charged track and the cluster is greater than  $18^\circ$ , the first hit is in the beginning six radiation lengths, the difference between the angle of the cluster development direction in the BSC and the photon emission direction is less than  $37^\circ$ , and the energy deposit in the shower counter is greater than 60 MeV.

#### 3.1 $J/\psi \rightarrow D_s^- e^+ \nu_e$ and $J/\psi \rightarrow D^- e^+ \nu_e$

Both  $J/\psi \rightarrow D_s^- e^+ \nu_e$  and  $J/\psi \rightarrow D^- e^+ \nu_e$  candidate decays must contain an  $e^+$ .  $D_s^-$  mesons are reconstructed in two modes  $D_s^- \rightarrow \phi\pi^-$  and  $K^- K^{*0}$ , with  $\phi \rightarrow K^+ K^-$  and  $K^{*0} \rightarrow K^+ \pi^-$ . The  $\phi$  candidates are reconstructed from two oppositely-charged kaons and must have an invariant mass  $|M_{KK} - 1.02| < 0.015 \text{ GeV}/c^2$ . The  $K^{*0}$  candidates are constructed from  $K^+$  and  $\pi^-$  candidates and are required to have an invariant mass in the range  $|M_{K\pi} - 0.896| < 0.060 \text{ GeV}/c^2$ .

$D^-$  candidates are reconstructed in the mode  $D^- \rightarrow K^+ \pi^- \pi^-$ . Candidate events are required to have four charged tracks which satisfy charged track

selection criteria, and the total charge of the tracks is required to be zero.

The polarization of the  $K^{*0}$  meson in  $D_s^-$  decay is also utilized to reject backgrounds by imposing a selection requirement on the helicity angle  $\theta_H$ . The helicity angle is defined as the angle between one of the decay products of the  $K^{*0}$  and the direction of the flight of  $K^{*0}$  in the  $K^{*0}$  rest frame. Background events are distributed uniformly in  $\cos\theta_H$  since they originate from random combinations, while signal events are distributed as  $\cos^2\theta_H$ . The  $K^{*0}$  candidates are required to have  $|\cos\theta_H| > 0.4$ . Fig. 2 shows the invariant mass distributions of  $K^+K^-$  and  $K^+\pi^-$  systems with arrows indicating the selection of  $\phi$  and  $K^*(892)$  candidates.

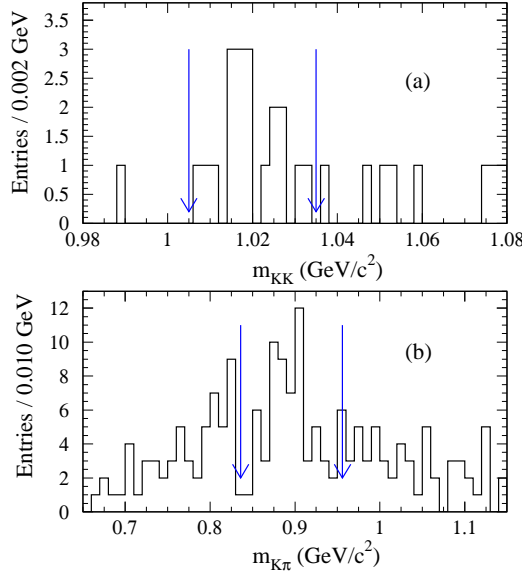


Fig. 2. (a)  $K^+K^-$  and (b)  $K^+\pi^-$  invariant mass distributions of  $D_s^- \rightarrow \phi\pi^-$ ,  $\phi \rightarrow K^+K^-$  and  $D_s^- \rightarrow K^-K^{*0}$ ,  $K^{*0} \rightarrow K^+\pi^-$  candidates. The signal regions for individual channels are indicated by arrows in the plot.

The angle between the identified electron and the nearest charged track is required to be larger than  $12^\circ$  to reject backgrounds from gamma conversions and  $\pi^0$  Dalitz decays. In order to reject backgrounds from  $J/\psi$  decaying to states with extra neutral particles, the number of isolated photons is constrained to be zero. The requirements for an isolated photon are more stringent than those for a good photon in order to increase the detection efficiency. An isolated photon is a photon with the angle between the nearest charged track and the cluster greater than  $22^\circ$  and the difference between the angle of the cluster development direction in the BSC and the photon emission direction less than  $60^\circ$ , and the energy deposit in the shower counter is greater than 0.1 GeV.

The four-momentum of the neutrino,  $p_\nu = (E_{miss}, \vec{p}_{miss})$ , is inferred from the difference between the net four momentum of the  $J/\psi$  particle,  $p_{J/\psi} =$

$(M_{J/\psi}, 0, 0, 0, )$ , and the sum of the four-momentum of all detected particles in the event.  $P_{miss}$  is required to be larger than 0.2 GeV/c and less than 0.9 GeV/c for  $J/\psi \rightarrow D_s^- e^+ \nu_e$  and larger than 0.2 GeV/c and less than 1.0 GeV/c for  $J/\psi \rightarrow D^- e^+ \nu_e$  to reduce background from  $J/\psi$  decay to 4-prong final states with misidentified particles but with no missing particles. We further require the absolute value of  $U_{miss}$ , which is defined as  $U_{miss} = E_{miss} - P_{miss}$ , to be less than 0.1 GeV, to reject backgrounds from  $J/\psi$  decaying to  $K_L^0$ ,  $\eta$ , and partially missing  $\pi^0$  final states, which were not rejected by prior criteria. After all requirements, the invariant mass distributions of  $D_s^- \rightarrow K^+ K^- \pi^-$  and  $D^- \rightarrow K^+ \pi^- \pi^-$  are shown in Figs. 3(a) and (b), respectively.

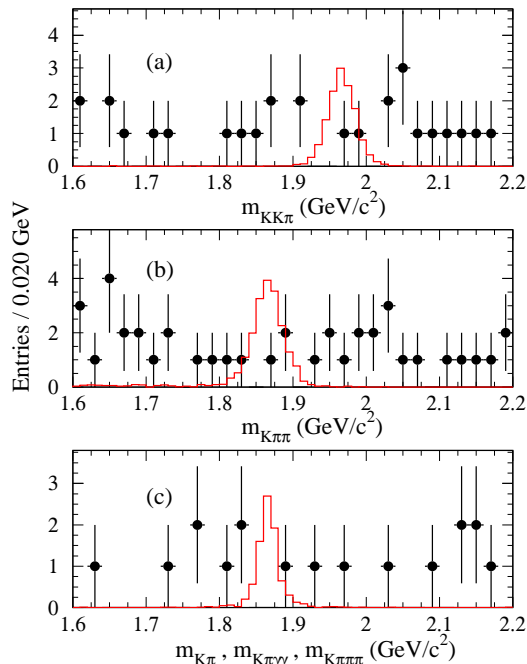


Fig. 3. Invariant mass distribution of (a)  $D_s^- \rightarrow K^+ K^- \pi^-$ , (b)  $D^- \rightarrow K^+ \pi^- \pi^-$ , and (c)  $\overline{D}^0 \rightarrow K^+ \pi^-, K^+ \pi^- \pi^0, K^+ \pi^- \pi^+ \pi^0$ . Data are shown by dots with error bars. The histogram is MC simulated signal events, unnormalized.

### 3.2 $J/\psi \rightarrow \overline{D}^0 e^+ e^-$

$\overline{D}^0$  mesons are reconstructed in three decay modes:  $\overline{D}^0 \rightarrow K^+ \pi^-$ ,  $\overline{D}^0 \rightarrow K^+ \pi^- \pi^0$ , and  $\overline{D}^0 \rightarrow K^+ \pi^- \pi^+ \pi^0$ . In  $\overline{D}^0 \rightarrow K^+ \pi^- \pi^0$ , the  $\pi^0$  candidates are reconstructed from a pair of photons. The  $\pi^0$  decay angle  $|E_{\gamma 1} - E_{\gamma 2}|/P_{\pi^0}$  is required to be  $< 0.9$  for  $K^+ \pi^- \pi^0$  in order to remove events in which the  $\pi^0$  is falsely reconstructed from a high-energy photon and a spurious shower. Here,  $P_{\pi^0}$  is the momentum of  $\pi^0$  and  $E_{\gamma 1}$  and  $E_{\gamma 2}$  are the energies of the two photons. Candidate events are required to have four or six charged tracks which satisfy the charged track selection criteria and total charge zero. Four-

constraint (4C) energy-momentum conservation kinematic fits are performed under the  $J/\psi \rightarrow e^+e^-K^+\pi^-$  or the  $J/\psi \rightarrow e^+e^-K^+\pi^-\pi^+\pi^-$  hypotheses, and the  $\chi^2_{4C}$  is required to be less than 15. The  $J/\psi \rightarrow e^+e^-K^+\pi^-\gamma\gamma$  hypothesis is subjected to a five-constraint (5C) fit where the invariant mass of the  $\gamma\gamma$  pair associated with the  $\pi^0$  is constrained to  $m_{\pi^0}$ , and  $\chi^2_{5C} < 15$  is required. For  $\overline{D}^0 \rightarrow K^+\pi^-\pi^0$ , if more than one combination of two good photons passes the kinematic fit, the combination with the smallest  $\chi^2$  is chosen. Gamma conversions and  $\pi^0$  Dalitz decays may produce electron-positron pairs with low electron-positron invariant mass. The requirement  $m_{ee} > 0.2 \text{ GeV}/c^2$  eliminates most of this type of background. The combined  $\overline{D}^0 \rightarrow K^+\pi^-, K^+\pi^-\pi^0, K^+\pi^-\pi^-\pi^+$  invariant mass distribution is shown in Fig 3(c).

## 4 Monte Carlo Simulation

Monte Carlo (MC) simulation is used for the determination of mass resolutions and detection efficiencies. We simulate  $J/\psi \rightarrow D_s^- e^+ \nu_e$ ,  $J/\psi \rightarrow D^- e^+ \nu_e$ , and  $J/\psi \rightarrow \overline{D}^0 e^+ e^-$  production and decay, including the detector response. In these simulations, 200000 events each are generated, and the decay branching fractions of  $D_s^-$ ,  $D^-$ , and  $\overline{D}^0$  are taken from the world average values [9]. The detection efficiencies and branching fractions obtained are listed in Table 1.

Table 1

Detection efficiencies and branching fractions [9].

Decay Mode	$\varepsilon_i$	$B_i$
$D_s^- \rightarrow \phi\pi^-(\phi \rightarrow K^+K^-)$	5.39%	$(3.6 \pm 1.1)\% \times (49.1 \pm 0.6)\%$
$D_s^- \rightarrow K^-K^{*0}(K^{*0} \rightarrow K^+\pi^-)$	4.29%	$(3.3 \pm 0.9)\% \times 2/3$
$D^- \rightarrow K^+\pi^-\pi^-$	8.67%	$(9.2 \pm 0.6)\%$
$\overline{D}^0 \rightarrow K^+\pi^-$	5.24%	$(3.80 \pm 0.09)\%$
$\overline{D}^0 \rightarrow K^+\pi^-\pi^0$	2.31%	$(13.0 \pm 0.8)\%$
$\overline{D}^0 \rightarrow K^+\pi^-\pi^-\pi^+$	2.15%	$(7.46 \pm 0.31)\%$

## 5 Systematic Errors

The largest systematic errors on the branching fraction measurements come from the uncertainties of the MDC simulation (including systematic uncertainties of the tracking efficiency) and the  $U_{miss}$  or kinematic fit requirements.

The photon detection efficiency has been studied with several different methods using  $J/\psi \rightarrow \rho^0 \pi^0$  decays [10]; the difference between data and Monte Carlo simulation is about 2% for each photon. We estimate a systematic error of 4% for  $\overline{D}^0 \rightarrow K^+ \pi^- \pi^0$ . The uncertainty for final states with no isolated photons is also studied using  $J/\psi \rightarrow \rho \pi$  decays and is about 2%. The systematic error from electron identification is estimated to be 5% for each electron. The pion and kaon identification is studied, and the difference between data and Monte Carlo simulation is 1.5% for each charged track, which is treated as a systematic error. The error on the intermediate decay branching fractions of  $D_s^-$ ,  $D^-$ ,  $\overline{D}^0$ ,  $\phi$ , and  $K^{*0}$  are taken from the PDG [9]. The statistical error of the Monte Carlo sample is taken into account. The total number of  $J/\psi$  events is  $(57.7 \pm 2.7) \times 10^6$  [11], determined from inclusive 4-prong hadronic final states, and the uncertainty, 4.7%, is taken as a systematic error. The systematic errors from all sources, as well as the total, are listed in Table 2.

Table 2

Summary of the systematic errors.

	$J/\psi \rightarrow D_s^- e^+ \nu_e$	$J/\psi \rightarrow D^- e^+ \nu_e$	$J/\psi \rightarrow \overline{D^0} e^+ e^-$		
	$D_s^- \rightarrow \phi \pi^-, K^- K^{*0}$	$D^- \rightarrow K^+ \pi^- \pi^-$	$\overline{D^0} \rightarrow K^+ \pi^-$	$K^+ \pi^- \pi^0$	$K^+ \pi^- \pi^- \pi^+$
MDC Simulation	18.6%	11.6%	20.6%		
Gamma	2.0%	2.0%	0.0%	4.0%	0.0%
$e$ PID	5.0%	5.0%	10.0%		
$\pi, K$ PID	4.5%	4.5%	3.0%	3.0%	6.0%
$B(D_s, D)$	25%	6.5%	2.4%	6.2%	4.2%
MC Statistics	5.1%	2.5%	2.7%		
number of $J/\psi$	4.7%				
total	32.7%	15.9%	23.8%	24.8%	24.6%

## 6 Results

No excess of  $J/\psi \rightarrow D_s^- e^+ \nu_e$ ,  $J/\psi \rightarrow D^- e^+ \nu_e$ , or  $J/\psi \rightarrow \overline{D}^0 e^+ e^-$  events above background is observed. The upper limit on the branching fractions of these decay modes are calculated using

$$B < \frac{n_{UL}^{obs}}{N_{J/\psi} \varepsilon B (1 - \sigma^{sys})}, \quad (1)$$

where  $n_{UL}^{obs}$  is the upper limit of the observed number of events at the 90% confidence level.  $N_{J/\psi}$  is the number of  $J/\psi$  events, and  $\varepsilon B$  is defined as  $\sum_{i=1}^N \varepsilon_i B_i$ , where  $\varepsilon_i$  and  $B_i$  are the detection efficiency and branching fraction for decay channel  $i$  and  $N$  is the number of decay modes, which are listed in Table 1. For instance, for  $J/\psi \rightarrow D_s^- e^+ \nu_e$ , the  $D_s^-$  mesons are reconstructed in two



decay modes, and  $N$  is equal to 2. The systematic error in the measurement is taken into consideration by introducing  $1 - \sigma^{sys}$  in the denominator of the branching fraction calculation.

We obtain upper limits for the observed number of events at 90% confidence level of 3.55 for  $J/\psi \rightarrow D_s^- e^+ \nu_e$ , 4.64 for  $J/\psi \rightarrow D^- e^+ \nu_e$  and 3.07 for  $J/\psi \rightarrow \overline{D^0} e^+ e^-$ , using a Bayesian method with uniform prior above zero [9]. The likelihood distributions and the 90% C.L. limits are shown in Fig. 4. The likelihood values for each value of the number of events are obtained by fitting the distributions shown in Fig. 3 with a signal shape determined from MC simulation and a second order polynomial to describe background. The upper limits are obtained from the integral of the normalized likelihood at the 90% confidence level. The numbers used in the branching fraction calculations are summarized in Table 3.

Table 3

Numbers used in the calculation of upper limits on the branching fractions of  $J/\psi \rightarrow D_s^-/D^- e^+ \nu_e + c.c.$  and  $J/\psi \rightarrow \overline{D^0} e^+ e^- + c.c.$ .

	$J/\psi \rightarrow D_s^- e^+ \nu_e + c.c.$	$J/\psi \rightarrow D^- e^+ \nu_e + c.c.$	$J/\psi \rightarrow \overline{D^0} e^+ e^- + c.c.$
$n_{UL}^{obs}$	3.55	4.64	3.07
$\varepsilon B$	$1.90 \times 10^{-3}$	$7.98 \times 10^{-3}$	$6.61 \times 10^{-3}$
Sys. Err.	32.7%	15.9%	24.8%
$B(90\%C.L.)$	$< 4.8 \times 10^{-5}$	$< 1.2 \times 10^{-5}$	$< 1.1 \times 10^{-5}$

In summary, we have searched for the decays  $J/\psi \rightarrow D_s^- e^+ \nu_e$ ,  $J/\psi \rightarrow D^- e^+ \nu_e$ , and  $J/\psi \rightarrow \overline{D^0} e^+ e^-$  using  $5.8 \times 10^7 J/\psi$  events acquired by the BESII detector at the BEPC  $e^+ e^-$  collider. No evidence for any of these decays is found. The final results for the 90% confidence level upper limit of the branching fractions are given in Table 3. The upper limits on the branching fraction for decays  $J/\psi \rightarrow D_s^- e^+ \nu_e$ ,  $J/\psi \rightarrow D^- e^+ \nu_e$ , and  $J/\psi \rightarrow \overline{D^0} e^+ e^-$  are not inconsistent with the standard model.

The BES collaboration thanks the staff of BEPC and computing center for their hard efforts. This work is supported in part by the National Natural Science Foundation of China under contracts Nos. 10491300, 10225524, 10225525, 10425523, the Chinese Academy of Sciences under contract No. KJ 95T-03, the 100 Talents Program of CAS under Contract Nos. U-11, U-24, U-25, and the Knowledge Innovation Project of CAS under Contract Nos. U-602, U-34 (IHEP), the National Natural Science Foundation of China under Contract No. 10225522 (Tsinghua University), and the Department of Energy under Contract No.DE-FG02-04ER41291 (U Hawaii).

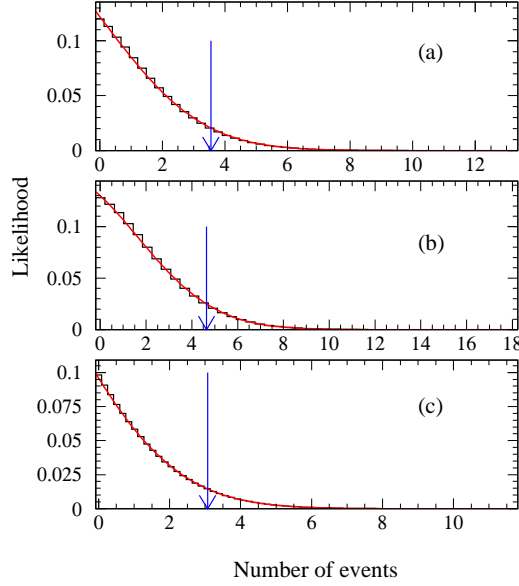


Fig. 4. Likelihood distributions for the observed number of events of (a)  $J/\psi \rightarrow D_s^- e^+ \nu_e$ , (b)  $J/\psi \rightarrow D^- e^+ \nu_e$ , and (c)  $J/\psi \rightarrow \overline{D}^0 e^+ e^-$ . The observed number of events at a Bayesian 90% confidence level for individual channels are indicated by arrows in the plots.

## References

- [1] Xinmin Zhang, High Energy Phys. Nucl. Phys. 25 (2001) 461.
- [2] C. Hill, Phys. Lett. B 345 (1995) 483.
- [3] Miguel Angel Sanchis-Lonzano, Z. Phys. C 62 (1994) 271.
- [4] BES Collaboration, J.Z. Bai, et al., Nucl. Instrum. Methods A 458 (2001) 627.
- [5] C. Zhang, et. al., in: J. Rossback(Ed.). HEACC'92 Hamburg, XVth International Conference on High Energy Accelerators, Hamburg, Germany, 20-24 July, 1992, p.409.
- [6] BES Collaboration, J.Z. Bai, et al., Nucl. Instrum. Methods A 344 (1994) 319.
- [7] BES Collaboration, M. Ablikim, et al., Nucl. Instrum. Methods A 552 (2005) 344.
- [8] S.S. Sun, K.L. He, et al., High Energy Phys. Nucl. Phys. 29 (2004) 162.(in Chinese)
- [9] Particle Data Group, S. Eidelman, et al., Phys. Lett. B 592 (2004) 1.
- [10] S.M. Li, et al., High Energy Phys. Nucl. Phys. 28 (2004) 859.(in Chinese)
- [11] S.S. Fang, et al., High Energy Phys. Nucl. Phys. 27 (2003) 277.(in Chinese)